scmap - A tool for unsupervised projection of single cell RNA-seq data

Vladimir Yu Kiselev[1] and Martin Hemberg[1]
[1] Wellcome Trust Sanger Institute, Hinxton, Cambridge, UK

Abstract

Single-cell RNA-seq (scRNA-seq) is widely used to investigate the composition of complex tissues[1–9] since the technology allows researchers to define cell-types using unsupervised clustering of the transcriptome[8,10]. However, due to differences in experimental methods and computational analyses, it is often challenging to directly compare the cells identified in two different experiments. Here, we present scmap (http://bioconductor.org/packages/scmap), a method for projecting cells from a scRNA-seq experiment onto the cell-types identified in other experiments (the application can be run for free, without restrictions, from http://www.hemberg-lab.cloud/scmap).

Main text

As more and more scRNA-seq datasets become available, carrying out comparisons between them is key. A central application is to compare datasets of similar biological origin collected by different labs to ensure that the annotation and the analysis is consistent (Fig. 1a). Moreover, as very large references, e.g. the Human Cell Atlas (HCA)[11], become available, an important application will be to project cells from a new sample (e.g. from a disease tissue) onto the reference to characterize differences in composition, or to detect new cell-types (Fig. 1b). Conceptually, such projections are similar to the popular BLAST[12] method, which makes it possible to quickly find the closest match in a database for a newly identified nucleotide or amino acid sequence.

Projecting a new cell, *c*, onto a reference dataset that has previously been grouped into clusters, amounts to identifying which cluster *c* is most similar to. We represent each cluster by its centroid, i.e. a vector of the median value of the expression of each gene, and we measure the similarity between *c* and each cluster centroid. Instead of using all genes when calculating the similarity, we use unsupervised feature selection to include only the genes that are most relevant for the underlying biological differences which allows us to overcome batch effects[13].

We investigate three different strategies for feature selection: random selection, highly variable genes (HVGs)[14] and genes with a higher number of dropouts than expected (M3Drop)[13]. To increase speed, we modified the M3Drop method and instead of fitting a Michaelis-Menten model to the log expression-dropout relation, we fit a linear model (Methods, Fig. S1a). For the number of features, we used the top 100, 200, 500, 1000, 2000, 5000, or all genes. Similarities were

calculated using the cosine similarity, Pearson and Spearman correlations. This has the advantage of being insensitive to differences in scale between datasets as the similarities are restricted to the interval [-1, 1]. To make the assignments more robust, we required that at least two of the three similarities were in agreement, and that their value exceeded .7 for at least one of them. If these criteria are not met, then *c* is labelled as "unassigned" to indicate that it does not correspond to any cell-type present in the reference.

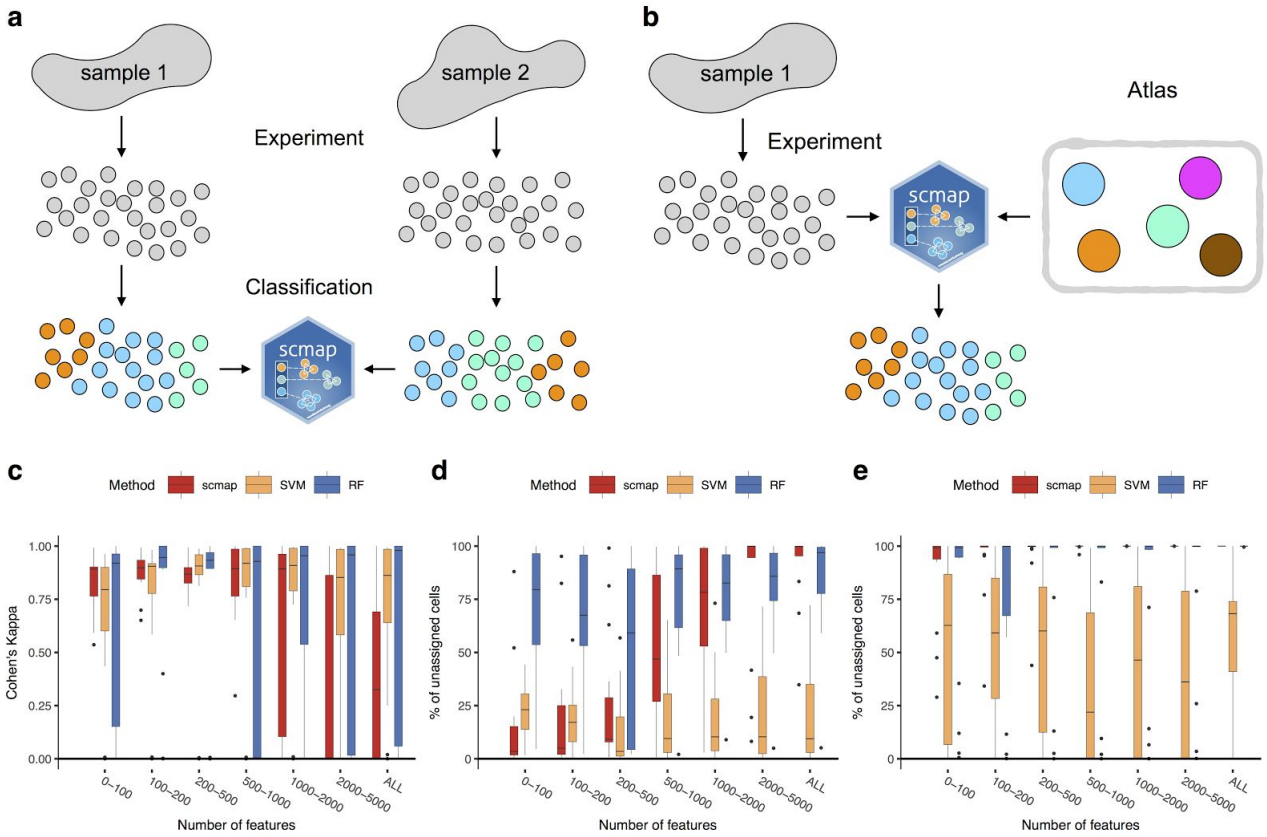

Figure 1 scmap use-cases and performance. (**a**) scmap can be used to compare the annotations of two different samples by providing a one to one mapping between the cells. (**b**) scmap can also be used to project cells from a new experiment onto an annotated reference. (**c**) Cohen's κ values and (**d**) percentage of unassigned cells for positive controls. The plots are based on seven pairs of datasets listed in Table S2 (projections are performed in both directions). Dropout-based feature selection is used for all three methods (see Methods). Colours are the same as in (**b**). (**e**) Percentage of unassigned cells in negative controls. The plot is based on nine pairs of datasets listed in Table S3 (projections are performed in both directions). Dropout-based feature selection is used everywhere (see Methods). Colours are the same as in (**b**).

To validate the projections, we considered 17 different datasets[1–9,15–21] from mouse and human, collected and processed in different ways (Table S1). First, we evaluated different feature selection methods by carrying out a self-projection experiment where each dataset is mapped onto itself. We used 70% of the cells from the original sample for the reference and the remaining 30% were projected, with clusters as defined by the original authors. To quantify the accuracy of the mapping, we use Cohen's κ[22] which is a normalized index of agreement between sets of labels that accounts for the frequency of each label. A value of 1 indicates that the projection assignments were in complete agreement with the original labels, whereas 0 indicates that the projection assignment was no better than random guessing. We find that the dropout-based

method for feature selection has the best performance, and somewhat surprisingly we also find that random selection is better than HVG (Fig. S1b). Furthermore, the dropout-based method performs consistently well when the number of features selected is in the range of [100, 1000]. As a comparison, we also considered two commonly used supervised methods for assigning labels to new samples, a random forests classifier (RF) and a support vector machine (SVM). These classifiers were trained on the reference and then applied to the held out cells as before. For the self-projection experiment, we find that both RF and SVM perform slightly better than scmap for all three feature selection methods.

As a positive control, we considered seven pairs of datasets (Table S2) that we expected to correspond well based on their origin. The positive controls represent a more realistic use-case since these comparisons include systemic differences between the reference and projection samples, i.e. batch effects. For example, for three of the pairs, one of the datasets was collected using a full-length protocol and the other was collected using a UMI based protocol. The results showed that despite the substantial differences between the protocols[15,23,24], scmap achieves κ>.75 and assignment rates >75% when the number of features used was between 100 and 500 (Fig. 1c, d, S2a, S3). Even though RF achieves the highest κ of the three approaches it also has the lowest assignment rate (< 50%) indicating it achieves a high specificity at the cost of low sensitivity.

As a negative control, we projected datasets with an altogether different origin from the reference (e.g. mouse retina onto mouse pancreas, Table S3). Reassuringly, we found that scmap categorized >90% of the cells as unassigned when the number of features used was >100 (Fig. 1e). Notably, SVM has a much smaller fraction of unassigned cells than RF and scmap, indicating that it is too lenient in assigning matches. Taken together, comparing the evidence across the self-projection experiments, the positive and negative controls, we conclude that scmap with 500 features provides the best performance balancing high sensitivity and specificity with a low false-positive rate.

An important feature of scmap is that it is very fast. It takes only around twenty seconds to select features and to calculate the centroids for 40,000 cells, whereas it takes almost thirty minutes to train using RF or SVM (Fig. 2a). For all three methods the time to project the new cells is negligible, which means they are very fast with a pre-computed reference. Since the complexity scales with the number of clusters in the reference, rather than the number of cells, scmap will be applicable to very large datasets. The scmap reference can easily be stored in memory since each cluster only requires a few hundred gene names and median values, making it suitable for real-time queries of large references.

Large references, including the HCA, will be an agglomeration of datasets collected by different groups. Merging different scRNA-seq datasets remains an open problem[25–27], but the results from our study suggest that samples with similar origin are largely consistent[28] (Fig. 1c). Instead of correcting for batches and merging, one can create a composite reference and compare the new cells to each dataset separately. When there are multiple datasets in the reference, scmap reports the best match for each dataset. Thus, if a cell shows a high degree of similarity to clusters with similar annotations from different datasets, that will increase the confidence of the mapping. To illustrate the mapping to multiple datasets, we considered the pancreas dataset by Baron *et al*[4]

since it had the most unassigned cells when projected to the other pancreas datasets (Fig. 2b). Combining all projections (Methods) we were able to reduce the fraction of unassigned cells from 99% (Xin) and 63% (Muraro) to 32% while slightly improving κ (Fig. 2c-d). Since the reference used by scmap is modular and can be extended without re-calculating the features or centroids for the datasets that have been processed previously, the strategy of not merging datasets is well suited for large references that are expected to grow over a long period of time.

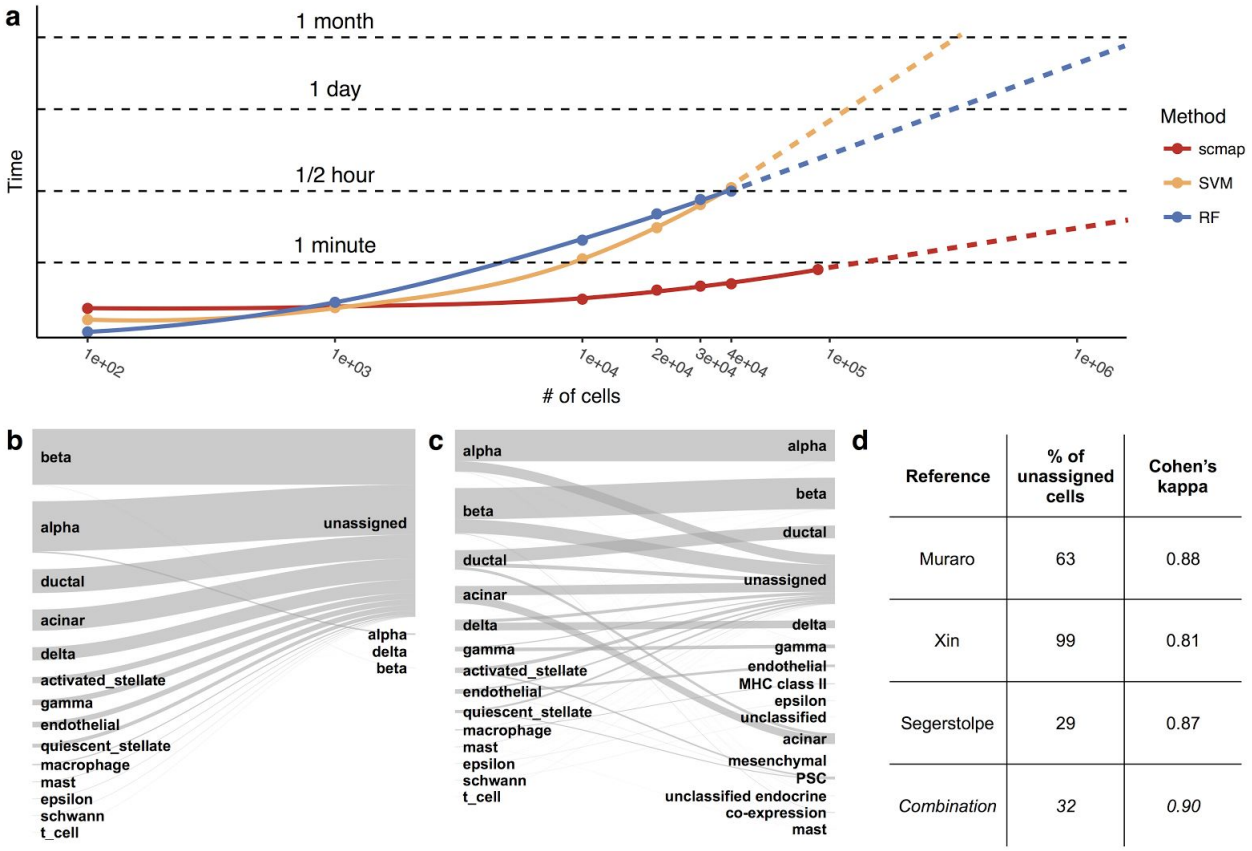

Reference	% of unassigned cells	Cohen's kappa
Muraro	63	0.88
Xin	99	0.81
Segerstolpe	29	0.87
Combination	*32*	*0.90*

Figure 2. scmap for combined references. (**a**) CPU run times of creating Reference (for scmap) and training classifiers (for SVM and RF). The x-axis represents a number of cells in the reference dataset. For all methods 1,000 features and 10,000 cells in the projection dataset were used. All methods were run on a MacBook Pro laptop (Mid 2014), OS X Yosemite 10.10.5 with 2.8 GHz Intel Core i7 processor, 16 GB 1600 MHz DDR3 of RAM. Points are actual data, solid lines are "loess" fit to the points with span = 1 (see ggplot2 documentation). Dashed lines are manual linear extrapolation of the solid lines. Results of scmap projection of the Baron et al[4] dataset to Xin et al[3] dataset (**b**) using one-to-one projection (Sankey diagram) and (**c**) to Muraro, Segerstolpe and Xin using a combination strategy (Sankey diagram). (**d**) Results of scmap projection of the Baron et al[4] dataset to three other human pancreas datasets (Reference) and results of the *Combination* projection.

We have implemented scmap as an R-package, and it is part of Bioconductor to facilitate incorporation into bioinformatic workflows. Since scmap is integrated with scater[29], it is easy to combine with many other popular computational scRNA-seq methods. Moreover, we have made scmap available via the web (http://www.hemberg-lab.cloud/scmap), allowing users to either upload their own reference, or to use a reference collection of datasets from this paper for which the features and centroids have been pre-calculated (Methods).

Due to differences in experimental conditions, comparing scRNA-seq datasets remains challenging. However, for researchers to be able to take advantage of large references, e.g. the HCA, a fast, robust and accurate method for projecting cells is required. To the best of our knowledge, scmap is the first such method. We have demonstrated that scmap can be used to compare samples of similar origin collected by different groups, as well as for comparing cells to a large reference composed of multiple datasets.

Methods

Datasets

All datasets and cell type annotations were downloaded from their public accessions. The datasets were converted into scater[29] objects (details are available on our dataset website: https://hemberg-lab.github.io/scRNA.seq.datasets). In Segerstolpe[1] dataset cells labeled as "not applicable" were removed. In Xin[3] dataset cell labeled as "alpha.contaminated", "beta.contaminated", "gamma.contaminated" and "delta.contaminated" were removed. In the following datasets similar cell types were merged together:

- In Deng[16] dataset *zygote* and *early2cell* were merged into *zygote* cell type, *mid2cell* and *late2cell* were merged into *2cell* cell type, and *earlyblast*, *midblast* and *lateblast* were merged into *blast* cell type.
- All bipolar cell types of the Shekhar[9] dataset were merged into *bipolar* cell type.
- In Yan[20] dataset *oocyte* and *zygote* cell types were merged into *zygote* cell type.

Feature selection

To select informative features we used a method conceptually similar to M3Drop[13] to relate the mean expression (E) and the dropout rate (D). Instead of modelling the relation between log(E) and D using Michaelis-Menten kinetics, we used a linear model to capture the relationship log(E) and log(D). After fitting a linear model using the lm() command in R, important features were selected as the top N residuals of the linear model (Fig. S1a). The features are only selected from the reference dataset, and those of them absent or zero in the projection dataset are are further excluded before the scmap mapping.

Reference centroid

In scmap each cell type in the reference dataset is represented by its centroid, i.e. the median value of gene expression for each feature gene across all cells in that cell type.

Projection dataset

Projection of a dataset to a reference dataset is performed by calculating similarities between each cell and all centroids of the reference dataset, using only the common selected features. Three

similarity measures are used: Pearson, Spearman and Cosine. The cell is then assigned to the cell type which correspond to the highest similarity value. However, scmap requires that at least two similarity measures agree with each other, otherwise the cell is marked as “unassigned”. Additionally, if the maximum similarity value across all three similarities is below a similarity threshold (default is .7), then the cell is also marked as “unassigned”. Positive and negative control plots corresponding to Figs. 1c-e for different values of the similarity/probability (see *SVM and RF*) threshold (.5, .6, .8 and .9) are shown in Fig. S2.

SVM and RF

scmap projection algorithm was benchmarked against support vector machines[30] (with a linear kernel) and random forests[31] (with 50 trees) classifiers from the R packages e1071 and randomForest. The classifiers were trained on all cells of the reference dataset and a cell type of each cell in the projection dataset was predicted by the classifiers. Additionally, a threshold (default value of .7) was applied on the probabilities of assignment: if the probability was less than the threshold the cell was marked as “unassigned”.

Projection based on multiple datasets

When the reference contains multiple datasets collected from similar samples by different groups in addition to all similarities, for each cell scmap also reports a top cell type match based on the highest value of similarities across all reference cell types. A similarity threshold of .7 is also applied in this case.

scmap on the Cloud

An example of a cloud version of scmap is available at http://www.hemberg-lab.cloud/scmap. Instructions of how to set it up on a user’s personal web cloud environment are available on our github page: https://github.com/hemberg-lab/scmap-shiny.

Figures

All data and scripts used to generate figures in this paper are available at https://github.com/hemberg-lab/scmap-paper-figures.

Acknowledgements

We would like to thank Tallulah Andrews, Kedar N Natarajan, Guillermo Parada, Michael Schaub, Michael Stubbington, Valentine Svensson, Jennifer Westoby and Florian Wünnermann for helpful discussions, feedback on the manuscript and for testing the cloud implementation of scmap.

Funding

Amazon Web Services (AWS) Cloud provided credits for running the scmap server for one year. VYK and MH were both supported by core funding to the Wellcome Trust Sanger Institute provided by the Wellcome Trust.

Conflicts of interest

None.

Author contributions

M.H. conceived the study and supervised the research; V.Y.K., M.H. contributed to the computational framework; V.Y.K. and M.H. wrote the manuscript.

References

1. Segerstolpe, Å. *et al.* Single-Cell Transcriptome Profiling of Human Pancreatic Islets in Health and Type 2 Diabetes. *Cell Metab.* **24,** 593–607 (2016).
2. Muraro, M. J. *et al.* A Single-Cell Transcriptome Atlas of the Human Pancreas. *Cell Syst* **3,** 385–394.e3 (2016).
3. Xin, Y. *et al.* RNA Sequencing of Single Human Islet Cells Reveals Type 2 Diabetes Genes. *Cell Metab.* **24,** 608–615 (2016).
4. Baron, M. *et al.* A Single-Cell Transcriptomic Map of the Human and Mouse Pancreas Reveals Inter- and Intra-cell Population Structure. *Cell Syst* **3,** 346–360.e4 (2016).
5. Zeisel, A. *et al.* Brain structure. Cell types in the mouse cortex and hippocampus revealed by single-cell RNA-seq. *Science* **347,** 1138–1142 (2015).
6. Tasic, B. *et al.* Adult mouse cortical cell taxonomy revealed by single cell transcriptomics. *Nat. Neurosci.* **19,** 335–346 (2016).
7. Usoskin, D. *et al.* Unbiased classification of sensory neuron types by large-scale single-cell RNA sequencing. *Nat. Neurosci.* **18,** 145–153 (2015).
8. Macosko, E. Z. *et al.* Highly Parallel Genome-wide Expression Profiling of Individual Cells Using Nanoliter Droplets. *Cell* **161,** 1202–1214 (2015).
9. Shekhar, K. *et al.* Comprehensive Classification of Retinal Bipolar Neurons by Single-Cell Transcriptomics. *Cell* **166,** 1308–1323.e30 (2016).
10. Kiselev, V. Y. *et al.* SC3: consensus clustering of single-cell RNA-seq data. *Nat. Methods* (2017). doi:10.1038/nmeth.4236
11. Regev, A. *et al.* The Human Cell Atlas. *bioRxiv* 121202 (2017). doi:10.1101/121202
12. Altschul, S. F., Gish, W., Miller, W., Myers, E. W. & Lipman, D. J. Basic local alignment search tool. *J. Mol. Biol.* **215,** 403–410 (1990).
13. Andrews, T. S. & Hemberg, M. Modelling dropouts for feature selection in scRNASeq experiments. *bioRxiv* 065094 (2017). doi:10.1101/065094

14. Brennecke, P. *et al.* Accounting for technical noise in single-cell RNA-seq experiments. *Nat. Methods* **10,** 1093–1095 (2013).
15. Klein, A. M. *et al.* Droplet Barcoding for Single-Cell Transcriptomics Applied to Embryonic Stem Cells. *Cell* **161,** 1187–1201 (2015).
16. Deng, Q., Ramsköld, D., Reinius, B. & Sandberg, R. Single-cell RNA-seq reveals dynamic, random monoallelic gene expression in mammalian cells. *Science* **343,** 193–196 (2014).
17. Goolam, M. *et al.* Heterogeneity in Oct4 and Sox2 Targets Biases Cell Fate in 4-Cell Mouse Embryos. *Cell* **165,** 61–74 (2016).
18. Pollen, A. A. *et al.* Low-coverage single-cell mRNA sequencing reveals cellular heterogeneity and activated signaling pathways in developing cerebral cortex. *Nat. Biotechnol.* **32,** 1053–1058 (2014).
19. Li, H. *et al.* Reference component analysis of single-cell transcriptomes elucidates cellular heterogeneity in human colorectal tumors. *Nat. Genet.* **49,** 708–718 (2017).
20. Yan, L. *et al.* Single-cell RNA-Seq profiling of human preimplantation embryos and embryonic stem cells. *Nat. Struct. Mol. Biol.* **20,** 1131–1139 (2013).
21. Kolodziejczyk, A. A. *et al.* Single Cell RNA-Sequencing of Pluripotent States Unlocks Modular Transcriptional Variation. *Cell Stem Cell* **17,** 471–485 (2015).
22. Cohen, J. Weighted kappa: nominal scale agreement with provision for scaled disagreement or partial credit. *Psychol. Bull.* **70,** 213–220 (1968).
23. Hashimshony, T. *et al.* CEL-Seq2: sensitive highly-multiplexed single-cell RNA-Seq. *Genome Biol.* **17,** 77 (2016).
24. Picelli, S. *et al.* Full-length RNA-seq from single cells using Smart-seq2. *Nat. Protoc.* **9,** 171–181 (2014).
25. Camp, J. G. *et al.* Multilineage communication regulates human liver bud development from pluripotency. *Nature* **546,** 533–538 (2017).
26. Tung, P.-Y. *et al.* Batch effects and the effective design of single-cell gene expression studies.

Sci. Rep. **7,** 39921 (2017).

27. La Manno, G. *et al.* Molecular Diversity of Midbrain Development in Mouse, Human, and Stem Cells. *Cell* **167,** 566–580.e19 (2016).
28. Crow, M., Paul, A., Ballouz, S., Josh Huang, Z. & Gillis, J. Addressing the looming identity crisis in single cell RNA-seq. *bioRxiv* 150524 (2017). doi:10.1101/150524
29. McCarthy, D. J., Campbell, K. R., Lun, A. T. L. & Wills, Q. F. Scater: pre-processing, quality control, normalization and visualization of single-cell RNA-seq data in R. *Bioinformatics* (2017). doi:10.1093/bioinformatics/btw777
30. Ben-Hur, A., Horn, D., Siegelmann, H. T. & Vapnik, V. Support Vector Clustering. *J. Mach. Learn. Res.* **2,** 125–137 (2002).
31. Breiman, L. Random Forests. *Mach. Learn.* **45,** 5–32 (2001).